Airgap Reluctance Identification for the Magnetic Equivalent Circuit Modelling of Induction Machines

J. Gyselinck[1] and R. V. Sabariego[2]
[1]BEAMS Department, Université Libre de Bruxelles (ULB), Belgium, email: johan.gyselinck@ulb.ac.be
[2]Dept. of Electrical Engineering and Computer Science (ACE), University of Liège, Belgium

***Abstract*—This paper focuses on the airgap reluctances that connect stator and rotor teeth in a Magnetic Equivalent Circuit (MEC) model of an induction machine. A dimensionless analytical expression is adopted for the position dependence of these reluctances, the three degrees of freedom of which are identified and validated by Finite Element (FE) modelling, considering a simplified geometry and the complete machine under study respectively. By way of validation the method is applied to a 3kW induction motor.**

***Index Terms*—Induction machines, magnetic equivalent circuits, harmonic distortion, finite element methods.**

I. Introduction

The 2-D FE method is a valuable tool for the electromagnetic analysis of electrical machines as it allows accounting for the machine's real geometry and winding scheme, global and local saturation, eddy current effects in the windings, etc. When many evaluations have to be performed (machine optimisation, analysis of control and fault detection algorithms, real-time simulation, etc.), FE modelling may become prohibitively expensive though. A MEC model offers then a good compromise between accuracy and computational cost [1-6]. In particular, compared to dq-type and winding-function models, harmonics due to slotting, saturation, eccentricity and faults (short circuits, broken bars, etc.), in flux linkages, currents and torque, are accounted for easily and reproduced with relatively high accuracy.

The equations governing a MEC model are mostly expressed in terms of nodal magnetic potential values; the associated system matrix contains permeances and all stator teeth may in principle be connected to all rotor teeth by nonzero or zero permeances (which readily allows considering skew) [1]. Compared to the nodal approach, the dual loop-flux (or mesh-flux) approach has the advantage of better numerical convergence, but at the expense of a less straightforward dynamic management of the airgap reluctances [6]. In this paper the loop-based MEC modelling of [4] is further developed, with particular attention to the identification of the airgap reluctances. The main added value concerns the coherent definition and calculation of these reluctances through FE modelling. This is illustrated and validated by considering a 3kW machine. The authors are not aware of a similar approach or study presented in literature. The extended paper will further deal with closed rotor slots and modelling of skew (single-slice vs. multi-slice MEC model) [4].

II. Identification of Airgap Reluctances

The basic MEC shown in Fig. 1 contains $2(N_s + N_r)$ flux loops, where N_s and N_r are the number of stator and rotor teeth respectively. Fig. 2 illustrates that a stator tooth and a rotor tooth are connected by a tooth-pair reluctance of (nonzero) permeance $\mathcal{P}_{\rm tp}$ if the corresponding tooth pitches overlap, i.e. when the misalignment x of the two teeth is smaller (in absolute value) than the average tooth pitch $\tau_{\rm av} = (\tau_{\rm s}+\tau_{\rm r})/2$; x is the distance between the centerlines of the teeth (shown in blue). This way there are exactly $N_s + N_r$ airgap reluctances and airgap flux loops, independently of the rotor position (Fig. 1). This network topology corresponds to non-crossing flux lines (and the flux density being divergence-free).

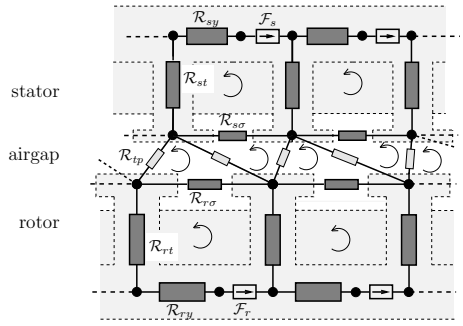

Fig. 1. Elementary MEC topology of an induction machine

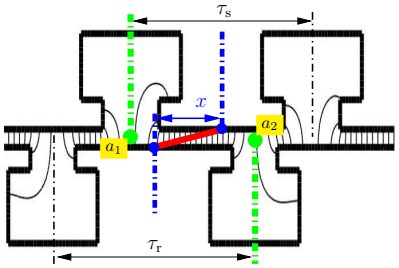

Fig. 2. Basic geometric parameters for an overlapping stator-rotor tooth pair (stator tooth pitch $\tau_{\rm s}$, rotor tooth pitch $\tau_{\rm r}$, misalignment coordinate x), the corresponding flux (delimited by the green dots, magnetic vector potential a_1 and a_2) and magnetomotive force (integral along red line between blue dots)

The flux going from the rotor tooth to the stator tooth, Φ, is by our definition the one delimited by the two center lines of the stator and rotor slot (green lines and dots in Fig.2). In case of a FE model, using the magnetic vector potential a, we have $\Phi = L_z(a_1 - a_2)$, where L_z is the axial length of the machine. The magnetomotive force $\mathcal{F}$ between the two teeth is obtained by integrating the magnetic field along a line (in red) connecting the two teeth. The permeance is then $\mathcal{P} = \Phi/\mathcal{F}$.

Misalignment x and permeance $\mathcal{P}_{\rm tp}$ are made dimensionless as follows: $x^* = x/\tau_{\rm av}$ and $\mathcal{P}^*_{\rm tp} = \mathcal{P}_{\rm tp}/(\mu_0\tau_{\rm av}/\delta)$, where μ_0 is the permeability of vacuum and δ the airgap width. The analytical function $\mathcal{P}^*_{\rm tp}(x^*)$ shown in Fig. 3 is adopted [4];

it is piecewise constant (interval $2d_1$), quadratic (twice d_2), linear (with slope ± 1, twice d_3) and quadratic (twice d_4). (The condition $d_1 + d_2 + d_3 + d_4 = 1$ is new compared to [4].) Notice the continuity of the derivative of $\mathcal{P}^*_{\rm tp}(x^*)$; this matters for the torque computation [1,4].

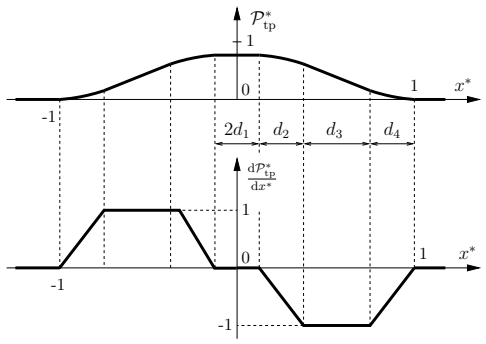

Fig. 3. Analytical $\mathcal{P}^*_{\rm tp}(x^*)$ curve and derivative $\frac{d\mathcal{P}^*_{\rm tp}}{dx^*}$

The more basic approach for fixing the $\mathcal{P}_{\rm tp}(x)$ relation consists in ignoring fringing flux [2,3], with possibly an increased equivalent airgap width (Carter factor correction). $\mathcal{P}_{\rm tp}(x)$ is then piecewise constant or linear, and its derivative discontinuous.

III. Application Example

We consider a 4-pole, 380/220 V, 50 Hz, 3 kW squirrel-cage induction motor with 36 stator slots and 32 rotor slots (Fig. 4) [4]. The commercial version of the rotor has 32 closed and skewed slots; three other rotors with open and/or unskewed slots have been constructed for research purposes. The noload and full-load stator current waveforms obtained with a (single-slice or multi-slice) FE or MEC model, with either of the four different rotors, agree well with the measured waveforms [4].

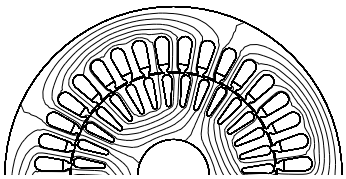

Fig. 4. Cross-section of 3 kW induction motor (full-load flux lines)

In this digest the study is limited to the unskewed rotor with open rotor slots, adopting either the actual 2 mm slot opening or a 4 mm one. A constant current is imposed in the three stator phases (1, -0.5 and 0.5 A resp.), and a zero current in all rotor bars (such that the torque is due to the slotting only). A constant and very large relative permeability (10^5) is assumed for the iron, in order to focus on the modelling of the airgap reluctances. A series of static calculations is carried out, with the FE and the MEC models, producing the results shown in Figs. 5 to 7.

From Fig. 5 it can be concluded that the proposed analytical form $\mathcal{P}^*_{\rm tp}(x^*)$ with 3 degrees of freedom is adequate, leading in Figs. 6 to 7 to a quite satisfactory prediction of the tooth harmonic in the rotor flux density and the torque. One further observes the effect of the plain airgap reluctance modelling (no fringing flux and no airgap width correction), i.e. a considerable under and overestimation of the fundamental flux component and the torque ripple respectively.

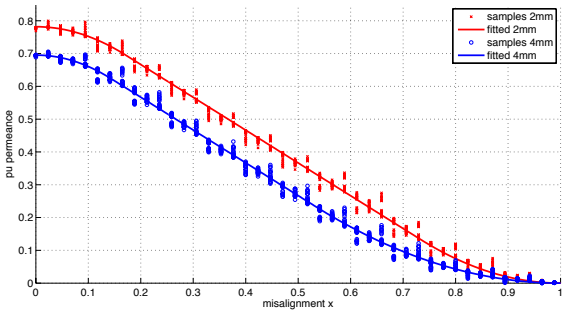

Fig. 5. $\{x^*, \mathcal{P}^*_{\rm tp}\}$ samples and fitted $\mathcal{P}^*_{\rm tp}(x^*)$ curves with 2 mm rotor slot opening (in red, $d_1 = 0$, $d_2 = 0.1693$, $d_3 = 0.5636$, $d_4 = 0.2671$) and 4 mm rotor slot opening (in blue, $d_1 = 0$, $d_2 = 0.1415$, $d_3 = 0.3912$, $d_4 = 0.5636$)

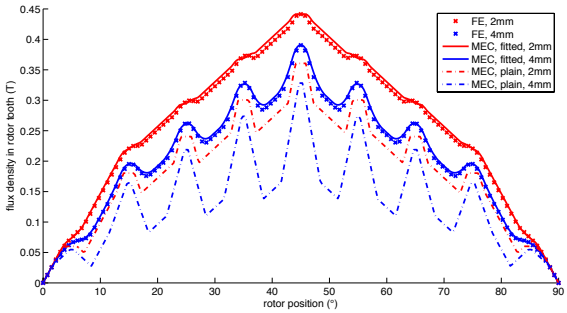

Fig. 6. Rotor tooth flux density versus rotor position (half electrical cycle)

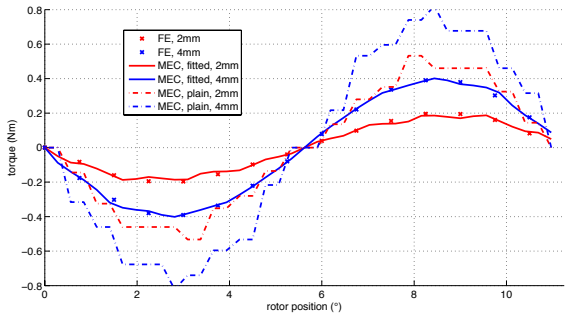

Fig. 7. Torque versus rotor position (one rotor tooth pitch)

References

[1] V. Ostovic, *Dynamic of saturated electric machines*, New York: Springer-Verlag, 1989.

[2] S. Sudhoff, B. Kuhn, K. Corzine, B. Branecky, "Magnetic equivalent circuit modeling of induction motors," *IEEE Trans. Energy Conversion*, vol. 22, no. 2, pp. 259–270, 2007.

[3] B. Asghari, V. Dinavahi, "Experimental validation of a geometrical nonlinear permeance network based real-time induction machine model," *IEEE Trans. Industrial Electronics*, vol. 59, no. 11, pp. 4049–4062, 2012.

[4] J. Gyselinck, J. Sprooten, X. Lopez-Fernandez, "Multi-slice FE modelling of induction motors having a broken bar - influence of inter-bar currents and bar breakage location," Proceedings of ICEM'2006.

[5] M. Bash, J. Williams, S. Pekarek, "Incorporating motion in mesh-based magnetic equivalent circuits," *IEEE Trans. Energy Conversion*, vol. 25, no. 2, pp. 329–338, 2010.

[6] G. Sizov, A. Sayed-Ahmed, Yeh Chia-Chou, N. Demerdash, "Analysis and diagnostics of adjacent and nonadjacent broken-rotor-bar faults in squirrel-cage induction machines," *IEEE Trans. Industrial Electronics*, vol. 56, no. 11, pp. 4627–4641, 2010.